Journal of Molecular Histology (2021) 52:173–185
https://doi.org/10.1007/s10735-020-09933-1

ORIGINAL PAPER

Circular RNA RBM33 contributes to cervical cancer progression via modulation of the miR-758-3p/PUM2 axis

Yi Ding[1,2] · Xia Yuan[1] · Wenwen Gu[1]

Received: 15 May 2020 / Accepted: 24 November 2020 / Published online: 5 January 2021

Abstract

Cervical cancer (CC) is a gynecological malignant tumor. Circular RNA (hsa_circ_0001772) (circRBM33) is implicated in the tumorigenesis of cancers. Nevertheless, the role of circRBM33 in CC is indistinct. Quantitative real-time polymerase chain reaction (qRT-PCR) was employed to evaluate the levels of circRBM33, miR-758-3p, and pumilio RNA binding family member 2 (PUM2) mRNA in tissue samples and cells. Cell proliferation, apoptosis, migration, invasion, and glycolysis were assessed using 3-(4, 5-dimethylthiazol-2-yl)-2, 5-diphenyltetrazolium bromide (MTT) assay, flow cytometry assay, transwell assay, or special commercial kits. Relative protein levels were examined via western blotting. The targeting relationship between circRBM33 or PUM2 and miR-758-3p was verified via dual-luciferase reporter or RNA pull-down assays. The role of circRBM33 was confirmed via tumor formation experiments. CircRPPH1 and PUM2 were upregulated while miR-758-3p was downregulated in CC tissues and cells. Functionally, circRBM33 knockdown constrained tumor growth in vivo and cured CC cell proliferation, migration, invasion, glycolysis, and fostered CC cell apoptosis in in vitro. Mechanistically, circRBM33 sponged miR-758-3p to modulate PUM2 expression. MiR-758-3p inhibitor neutralized circRBM33 silencing-mediated effects on the malignant behaviors of CC cells. PUM2 elevation overturned the suppressive influence of miR-758-3p upregulation on the malignant behaviors of CC cells. CircRBM33 fostered CC advancement via absorbing miR-758-3p and upregulating PUM2, indicating that circRBM33 was a possible target for CC treatment.

Keywords CC · circRBM33 · miR-758-3p · PUM2

Introduction

Cervical cancer (CC) is a malignant tumor of the uterine cervix, which ranks fourth among common cancers and cancer-related causes of death in women (Bray et al. 2018; Zhang et al. 2018a, b). Currently, the treatment of CC includes surgery, radiotherapy, and chemotherapy, but some patients are resistant to chemotherapy drugs, resulting in poor treatment results (Kodama et al. 2010; Rischin et al. 2010). At present, there is a need to develop new treatments for CC (Zhang et al. 2018a, b). Hence, it is indispensable to explore the molecular mechanism of CC development to provide a basis for the development of clinical treatment strategies (Rui et al. 2018).

Circular RNAs (circRNAs) are a type of non-coding RNAs with covalent circular structures that can function as transcription factors, microRNA (miRNA) sponges, and protein-like regulators (Hsiao et al. 2017). A large number of circRNAs are cell-specific and participate in the physiological development of organisms and the occurrence and advancement of diseases (Chen and Huang 2018). For example, circRNA has_circ_100395 was downregulated in lung cancer, and its overexpression impeded lung cancer progression via regulation of the miR-1228/TCF21 axis (Chen et al. 2018). Circular RNA hsa_circ_0001772 (circRBM33) is transcribed from the exons of the RBM33 (RNA binding motif protein 33) gene (http://www.circbank.cn/search.html?selectValue=hsa_circ_0001772). It was reported that circRBM33 contributed to the progression of gastric cancer (Wang

✉ Yi Ding
ia83qxx@163.com

[1] Department of Obstetrics & Gynaecology, the Affiliated Jintan Hospital of Jiangsu University, Changzhou 213200, People's Republic of China

[2] Department of Obstetrics & Gynaecology, The Affiliated Jintan Hospital of Jiangsu University, No. 16, Nanmen Street, Jintan District, Changzhou City, Jiangsu Province, People's Republic of China

et al. 2020). However, the function and regulatory mechanism of circRBM33 in CC are unclear.

MiRNAs usually impede the translation and stability of messenger RNAs, which are related to cellular processes, such as stress response, cell cycle regulation, inflammation, migration, differentiation, and apoptosis (Di Leva et al. 2014). Functional researches have confirmed that miRNAs play a role as tumor suppressors or oncogenes in a range of tumors (Rupaimoole et al. 2017). For instance, miR-93 and miR-106b accelerated breast cancer progression via activating the PI3K/AKT pathway by targeting PTEN (Li et al. 2017). MiRNA-758-3p (miR-758-3p) had been reported to exert an inhibitory role in diverse tumors, including bladder cancer (Wu et al. 2019a, b), papillary thyroid cancer (Chen et al. 2019), ovarian cancer (Hu et al. 2019), and so on. Previous researches revealed that miR-758-3p was connected with the development of CC (Meng et al. 2017; Song et al. 2019). Nevertheless, the exact mechanism of CC advancement associated with miR-758-3p is still indistinct.

The protein encoded by the pumilio RNA binding family member 2 (PUM2) gene is an RNA binding protein. In glioblastoma, PUM2 could facilitate cancer cell migration and proliferation (Wang et al. 2019). Moreover, PUM2 played a promoting influence on the stemness of breast cancer cells (Zhang et al. 2019). Also, TUG1 promoted CC advancement through upregulating PUM2 (Duan et al. 2019).

The study aimed to survey the role and regulatory mechanism of circRBM33 in CC progression. The results revealed that circRBM33 facilitated CC development by regulating the miR-758-3p/PUM2 axis.

Materials and methods

CC specimens

The research was authorized and supervised by the ethics committee of the Affiliated Jintan Hospital of Jiangsu University. 55 paired CC tissues and neighbor non-cancer tissues were collected form the Affiliated Jintan Hospital of Jiangsu University. All patients who participated in the study had signed informed consents and did not receive radiotherapy, chemotherapy, or hormone therapy before surgery. The clinical characteristics of CC patients were exhibited in Table 1.

Cell culture and transfection

Human CC cells (HeLa and SiHa) and normal cervical epithelial cells ECt1/E6E7 were bought from the American Type Culture Collection (ATCC, Manassa, VA, USA). All cells were cultured in Dulbecco's Modified Eagle's Medium (DMEM) (Sigma, St Louis, MO, USA) supplemented with 10% fetal bovine serum (FBS, Life Technologies, Carlsbad, CA, USA), streptomycin (100 g/mL, Sigma), and penicillin (100 U/mL, Sigma) at 37 °C under an atmosphere containing 5% CO_2.

Small interference (si) RNA targeting circRBM33 (si-circRBM33: 5′-UACAUGAACUUGAAGAUGATT-3′), negative control (si-NC: 5′-AUGAAUUUACAUGAACUUGTT3′), and the lentivirus vector carrying sh-circRBM33 or sh-NC were achieved from Genepharma (Shanghai, China). MiR-758-3p mimics and inhibitors (miR-758-3p and anti-miR-758-3p) and their matching controls (miR-NC and anti-miR-NC) were obtained from Ribobio (Guangzhou,

Table 1 Correlations between circRBM33 expression and clinical characteristics in cervical cancer patients (n = 55)

Clinicopathologic parameters	Case	circRBM33 expression		*P* value[a]
		Low (n = 27)	High (n = 28)	
Age (years)				0.5076
≤ 45	24	13	11	
> 45	31	14	17	
Tumor size				0.0025*
≤ 4 cm	36	23	13	
> 4 cm	19	4	15	
FIGO stage				0.0323*
Ib	35	21	14	
IIa–IIb	20	6	14	
Lymph node metastases				0.0032*
Present	21	5	16	
Absent	34	22	12	

*$P < 0.05$

[a]Chi-square test

China). The pcDNA3.1-PUM2 (PUM2) vector was obtained by cloning the sequence of PUM2 into the pcDNA3.1 vector (vector) (Life Technologies). The specified vectors and/or oligonucleotides were transfected into CC cells with the Lipofectamine 3000 reagent (Life Technologies).

Quantitative real-time polymerase chain reaction (qRT-PCR)

Total RNA was extracted from tissue specimens and cells with the TRIzol reagent (Sigma). For reverse transcription, total RNA (25 μL) was transcribed into complementary DNA using the High-Capacity complementary DNA Reverse Transcription Kit (Applied Biosystems, Foster City, CA, USA) or MicroRNA Reverse Transcription Kit (Applied Biosystems). QRT-PCR was conducted with the SYBR Green PCR Master Mix (Applied Biosystems). The expression of circRBM33, RBM33, miR-758-3p, and PUM2 were calculated using the $2^{-\Delta\Delta Ct}$ method, and glyceraldehyde-3-phosphate dehydrogenase (GAPDH) or U6 small nuclear RNA (U6) was used as the internal control. Primers were exhibited as below: circRBM33 (F: 5′-TGTAACACCCTGAGAACTGAAAT-3′, R: 5′-GAGTGACAGGACGCACTCAG-3′), GAPDH (F: 5′-GAAGGTGAAGGTCGGAGTC-3′, R: 5′-GAAGATGGTGATGGGATTTC-3′), RBM33 (F: 5′-CACATCAACCCGCACTTCAAA-3′, R: 5′-GAACAGGTCCAGGTGTATGCT-3′), miR-758-3p (F: 5′-ACACTCCAGCTGGGTTTGTGACCTGGTCCA-3′, R: 5′-CTCAACTGGTGTCGTGGAGTCGGCAATTCAGTTGAGGGTTAGTG-3′), PUM2 (F: 5′-TTCCACAGCCAAGAGACGCA-3′, R: 5′-GCACTCAGCCACCACAGCAG-3′), and U6 (F: 5′-GCTTCGGCAGCACATATACTAAAAT-3′, R: 5′-CGCTTCACGAATTTGCGTGTCAT-3′).

RNase R and Actinomycin D treatment

For RNase R treatment, total RNA of CC cells were treated with RNase R (3 U/μg, Epicentre Technologies, Madison, WI, USA) at 37 °C for 15 min. To prevent CC cell transcription, Actinomycin D (2 mg/mL, Sigma) was added to the medium. The levels of circRBM33 and RBM33 mRNA were evaluated via qRT-PCR.

Subcellular distribution assay

The PARIS kit (Life Technologies) was employed to extract the nuclear and cytoplasmic RNAs from CC cells based on the manufacturer's instructions. The levels of circRBM33 were assessed via qRT-PCR, and GAPDH or U6 were used as an internal control for cytoplasm RNA and nucleus RNA.

Cell proliferation assay

After transfection with vectors or oligonucleotides, CC cells (3.0×10^3 cells/well) were seed into 96-well plates and cultured for 24 h, 48 h, and 72 h under the right conditions. Then, 3-(4, 5-dimethylthiazol-2-yl)-2, 5-diphenyltetrazolium bromide (MTT) solution (20 μL, 5 mg/mL, Sigma) was added to each well. Subsequently, the crystals were dissolved using dimethyl sulfoxide (150 μL). The color reaction at 490 nm was determined using a Microplate Absorbance Reader (Bio-Rad, Hercules, CA, USA).

Flow cytometry assay

Cell apoptotic rate was evaluated with an Annexin V-FITC-propidium iodide (PI) kit (BD Biosciences, San Diego, CA, USA). In short, the transfected CC cells were harvested after culture for 48 h. Next, the cells (1.0×10^6 cells/mL) were placed to a precooled ethanol solution (70%) overnight at 4 °C. Subsequently, the cells (100 μL) were re-suspended in binding buffer (200 μL), and then stained with Annexin V-FITC (10 μL) and PI (5 μL). Thereafter, the apoptosis of transfected CC cells was detected with the FACScan® flow cytometry (BD Biosciences).

Transwell assay

Cell migration was analyzed with the transwell chamber (Costar, Cambridge, MA, USA). Briefly, DMEM containing transfected CC cells (100 μL, 1.0×10^6 cells/mL) was added to the upper chamber. The DMEM with FBS (10%) was added to the lower chamber. After culture for 24 h, the cells on the lower surface of the chamber were fixed with 5% glutaraldehyde and stained with crystal violet (0.1%, Sigma). For the invasion assay, its procedure was the same method as the migration assay, but the transwell chamber used was pre-covered with Matrigel (BD Biosciences). The number of migrated and invasive cells was determined with an inverted microscope (Bio-Rad).

Western blotting

Total protein of tissue specimens and cells was extracted using the lysis buffer (Beyotime, Shanghai, China). Western blotting was performed as described previously (Ren et al. 2019). The immunoblot was visualized using the enhanced chemiluminescence solution (Beyotime). The primary antibodies used in the research were exhibited as blow: anti-E-cadherin (ab15148, 1:2000, Abcam, Cambridge, MA, USA), anti-N-cadherin (ab76057, 1:1000, Abcam), and anti-Vimentin (ab137321, 1:1000, Abcam), anti-Hexokinase II (HK2) (ab227198, 1:5000, Abcam), anti-PUM2 (ab92390, 1:1000, Abcam), and anti-GAPDH (ab9484, 1:1000, Abcam). Goat

anti-rabbit IgG (ab97051, 1:1000, Abcam) and GAPDH was used as a secondary antibody and loading control, respectively.

Measurement of glucose consumption and lactate production

The concentrations of glucose and lactate in the cell medium were determined through the glucose or lactate assay kits (BioVision, Milpitas, CA, USA) according to the manufacturer's instructions. The glucose consumption was the difference in glucose concentration between the original medium and the cell medium.

Dual-luciferase reporter assay

The potential binding sites between circRBM33 or PUM2 and miR-758-3p were predicted through the circInteractome or targetscan databases. The sequences of circRBM33 wild type (WT), circRBM33 mutant (MUT), PUM2 3′-UTR (Untranslated Regions)-WT, and PUM2 3′-UTR-MUT were synthesized and inserted into the psiCHECK-2 plasmids (Promega, Madison, WI, USA) to establish the luciferase reporter plasmids, respectively. CC cells were co-transfected with a luciferase reporter plasmid and miR-758-3p mimic or miR-NC with the Lipofectamine 3000 (Life Technologies). The luciferase activities were assessed with the dual-luciferase reporter assay system (Promega). The relative activity of luciferase reporter vectors was judged by evaluating the ratio of firefly luciferase activity to Renilla luciferase activity.

RNA pull-down assay

In short, CC cells were transfected with biotinylated (biotin)-miR-758-3p (Sigma) or biotin-NC (Sigma). The cells were collected and lysed after transfection for 48 h. Next, the biotin-labeled miRNA was pulled down by incubating with C-1 magnetic beads (Life Technologies). The bound RNA was purified through the TRIzol reagent (Sigma). The enrichment of circRBM33 was evaluated with qRT-PCR.

Tumor formation experiments

The tumor formation experiments were conducted as described previously (Feng et al. 2019). The protocols of tumor formation experiments were approved by the Animal Ethics Committee of the Affiliated Jintan Hospital of Jiangsu University. In brief, HeLa cells (5.0×10^6 cells/0.2 mL PBS) infected with lentivirus vector carting sh-circRBM33 or sh-NC were subcutaneously injected into the right flank of each BALB/c nude mice (5-week-old, Experimental Animal Center, Shanghai, China), 5 mice in each group. All nude were fed under Specific Pathogen Free conditions. The tumor formation experiments were carried out in the Affiliated Jintan Hospital of Jiangsu University. Tumor volume was measured every once a week using a caliper and calculated with the equation: Volume = (length × width^2)/2. 35 days later, all mice were killed via cervical dislocation under 5% isoflurane for subsequent analysis.

Statistical analysis

The data in the research were exhibited as mean ± standard deviation and acquired through 3 repeated experiments. SPSS 20.0 software (IBM, Armonk, NY, USA) was utilized for statistical analysis. The normal distribution was assessed through a Kolmogorov-Smirnov test. The correlations between circRBM33 expression and clinicopathological features were analyzed with Chi-sequre test. Paired Student's *t* test was applied to evaluate the differences in the paired samples, while the independent Student's *t* test was utilized for the evaluation of the differences between 2 independent groups. The variance homogeneity was analyzed by F-test. One-way variance analysis with hoc post Turkey test was utilized for the comparison of the differences among more groups. Differences were deemed significant if $P < 0.05$.

Results

CC patients with high circRBM33 expression had a poor prognosis

At the outset, we analyzed the microarray data (GEO accession: GSE102686) and discovered that circRBM33 expression was increased in CC tissues relative to the normal tissues (Fig. 1a). CircRBM33 (circBase ID: hsa_circ_0001772), transcribed from the exons (3–5) of the RBM33 gene, is located on chr7:155,465,560–155,473,602 and its spliced length is 445 bp (Fig. 1b). Subsequently, we verified the expression of circRBM33 in 55 pairs of CC tissues and neighbor non-cancer tissues. QRT-PCR presented that circRBM33 was upregulated in CC tissues in comparison to neighbor non-cancer tissues (Fig. 1c). Also, circRBM33 was highly expressed in CC cells (HeLa and SiHa) than that in ECt1/E6E7 cells (Fig. 1d). Statistical analysis manifested that high circRBM33 expression was associated with tumor size ($P = 0.0025$), FIGO stage ($P = 0.0323$), and lymph node metastases ($P = 0.0032$) (Table 1). Kaplan-Meier survival curve analysis exhibited that there was a shorter overall survival in CC patients with high expression of circRBM33 compared to those with low expression of circRBM33 (Fig. 1e). Furthermore, the half-time of linear RBM33 was less than 8 h, while circRBM33 was more than 24 h (Fig. 1f, g). Also, RBM33 mRNA can be digested

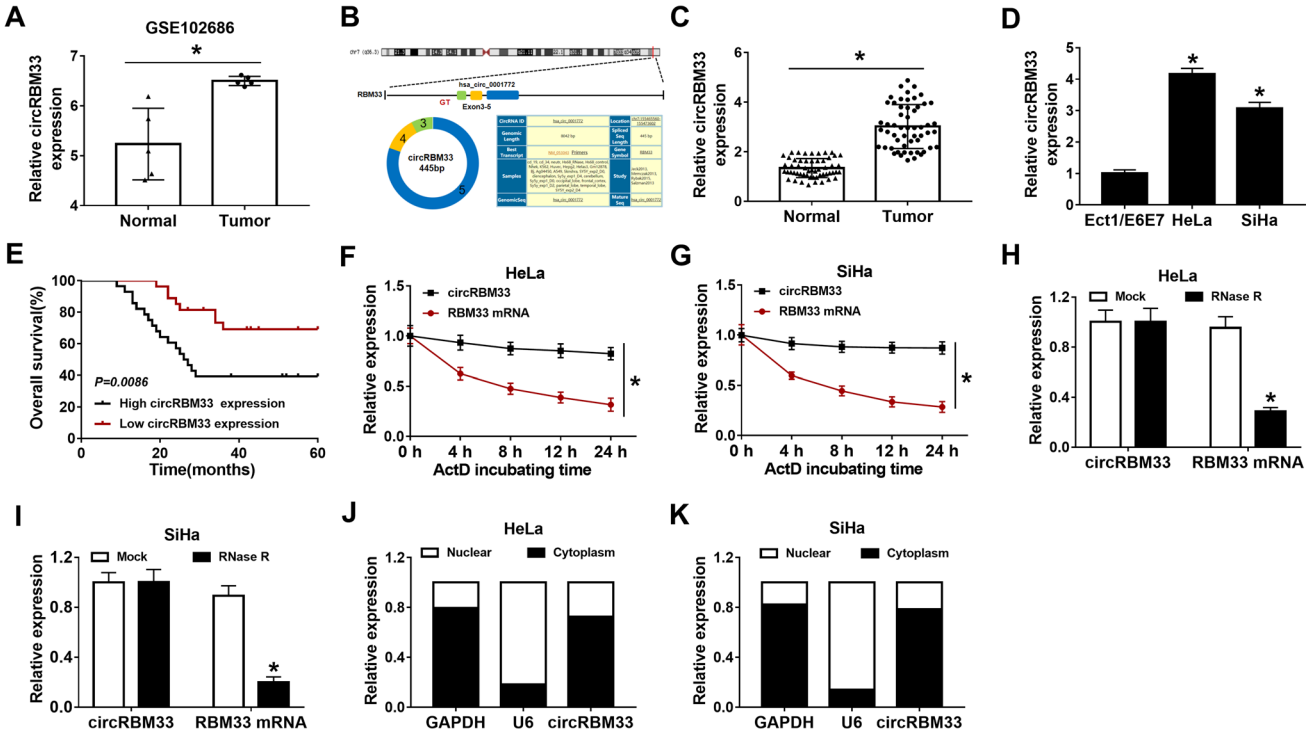

Fig. 1 CircRBM33 was upregulated in CC tissues and cells. **a** Scatter plots exhibited the expression of circRBM33 in CC tissues compared with adjacent normal tissues from the GSE102686 dataset. **b** Schematic displayed that circRBM33 was generated from the exons (3–5) of the RBM33 gene. **c** and **d** QRT-PCR was performed to assess the expression of circRBM33 in CC tissues and cells (HeLa and SiHa). **e** Kaplan-Meier survival plots exhibited the overall survival of CC patients with high or low expression of circRBM33. **f**–**i** The expression of circRBM33 and RBM33 mRNA in HeLa and SiHa cells treated with actinomycin D or RNase R was analyzed via qRT-PCR. **j**–**k** The subcellular distribution of circRBM33 was analzyed through qRT-PCR. $^*P < 0.05$

by RNase R treatment, while circRBM33 was not affected (Fig. 1h, i). Subcellular distribution assay exhibited that circRBM33 was preferentially localized in the cytoplasm of HeLa and SiHa cells (Fig. 1j, k). These results indicated that circRBM33 might play vital roles in CC progression.

CircRBM33 accelerated CC cell malignancy and glycolysis in vitro

To investigate the function of circRBM33 in CC, we performed loss-of-function experiments. The results exhibited that circRBM33 expression was apparently reduced in HeLa and SiHa cells transfected with si-circRBM33 in contrast to the control si-NC (Fig. 2a, b). Next, MTT assay revealed that circRBM33 inhibtion constrained cell proliferation in HeLa and SiHa cells (Fig. 2c, d). Flow cytometry assay indicated that circRBM33 downregulated increased the apoptotic rate of HeLa and SiHa cells (Fig. 2e). Transwell assay exhibited that circRBM33 knockdown impeded the migration and invasion abilities of HeLa and SiHa cells (Fig. 2f, g). The protein levels of N-cadherin and Vimentin were decreased in circRBM33-silenced HeLa and SiHa cells, but the protein level of E-cadherin had an opposing tendency (Fig. 2h, i). In addition, we observed that the levels of glucose consumption and lactate production were reduced in si-circRBM33-transfected HeLa and SiHa cells (Fig. 2j, k). The level of HK2 protein was also downregulated in si-circRBM33-transfected HeLa and SiHa cells (Fig. 2l, m). These findings revealed that circRBM33 exerted a promoting influence on the malignant behaviors and glycolysis of CC cells.

CircRBM33 acted as a sponge for miR-758-3p in CC cells

To explore whether circRBM33 can function as "miRNA sponge" in CC cells, we predicted the potential miRNAs that could bind to circRBM33 using the circInteractome database. The results presented that miR-758-3p possessed the possible binding sites for circRBM33 (Fig. 3a). Dual-luciferase reporter assay manifested that miR-758-3p overexpression could reduce the luciferase activity of the luciferase vector with circRBM33 WT in HeLa and SiHa cells but not the luciferase vector with circRBM33 MUT (Fig. 3b, c). RNA pull-down assay displayed that circRBM33 could be pulled down by the biotin-miR-758-3p probe in HeLa and SiHa cells rather than the biotin-NC

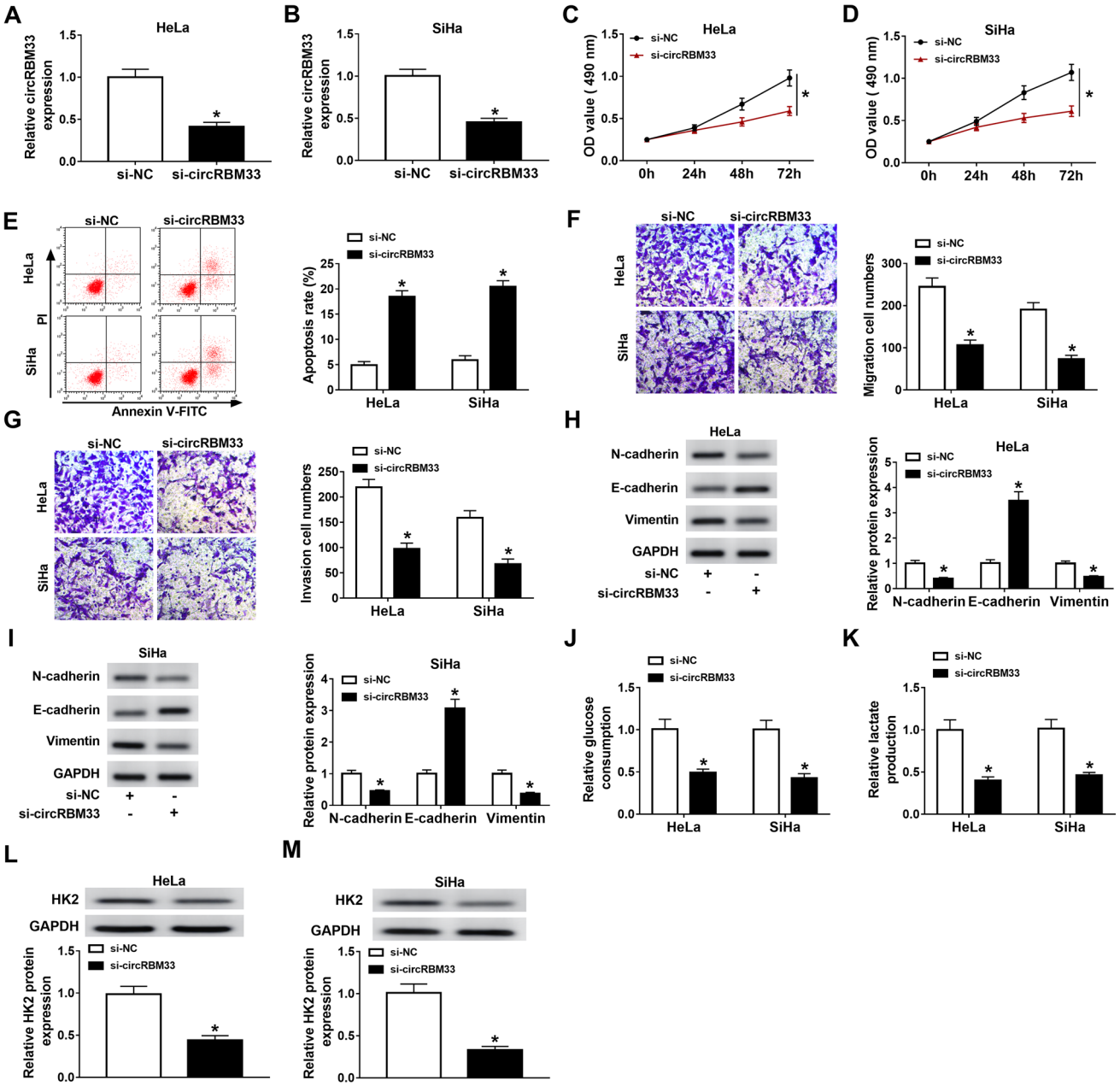

Fig. 2 Influence of circRBM33 on the malignancy and glycolysis of CC cells. **a**, **b** The knockdown efficiency of circRBM33 in HeLa and SiHa cells was verified by qRT-PCR. **c**–**g** Influence of circRBM33 silencing on proliferation, apoptosis, migration, and invasion of HeLa and SiHa cells was analyzed via MTT assay, flow cytometry assay, or transwell assay. The magnification of the transwell picture was ×100. **h**, **i** The levels of E-cadherin, N-cadherin, and Vimentin in circRBM33-repressed HeLa and SiHa cells were detected with western blotting. **j**, **k** The levels of glucose consumption and lactate production in circRBM33-repressed HeLa and SiHa cells were measured via special commercial kits. **l**, **m** The level of HK2 protein in circRBM33-repressed HeLa and SiHa cells were evaluated by western blotting. $^{*}P < 0.05$

(Fig. 3d). Furthermore, miR-758-3p expression was reduced in CC tissues and cells (HeLa and SiHa) (Fig. 3e, f). Also, circRBM33 knockdown elevated the expression of miR-758-3p in HeLa and SiHa cells (Fig. 3g). These findings indicated that circRBM33 served as a miRNA sponge for miR-758-3p in CC cells.

CircRBM33 modulated CC cell malignancy and glycolysis by absorbing miR-758-3p in vitro

Given that circRBM33 acted as a sponge for miR-758-3p in CC cells, we further analyzed whether circRBM33 absorbed miR-758-3p to regulate the advancement of CC. We

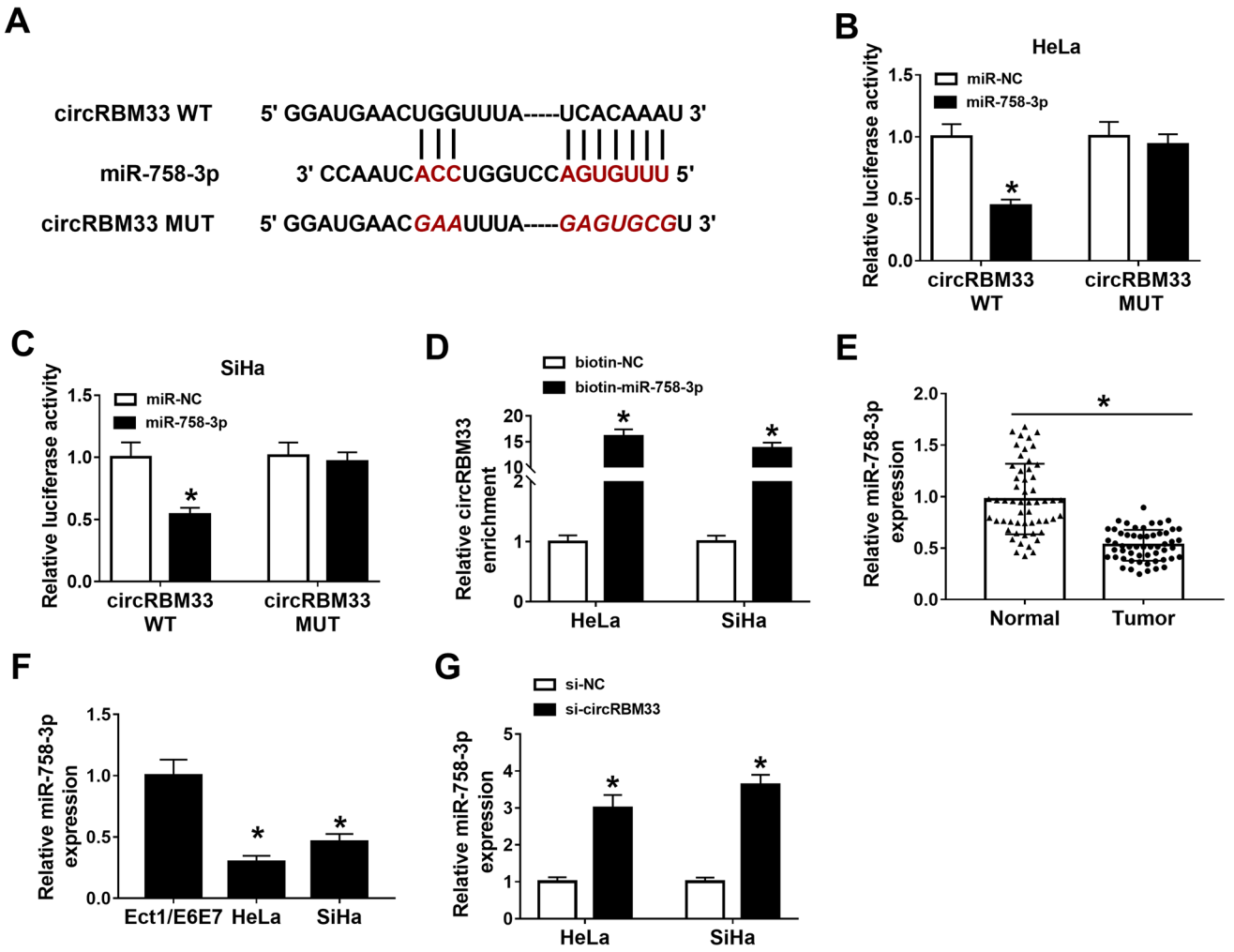

Fig. 3 CircRBM33 served as a sponge for miR-758-3p in CC cells. **a** Schematic diagram of the binding sites between miR-758-3p and circRBM33. **b**, **c** The luciferase intensity of the luciferase vector containing circRBM33 WT or circRBM33 MUT in HeLa and SiHa cells transfected with miR-NC or miR-758-3p was determined with dual-luciferase reporter assay. **d** After RNA pull down assay, the enrichment of circRBM33 was analyzed through qRT-PCR. **e**, **f** The expression of miR-758-3p in CC tissues and cells was evaluated through qRT-PCR. **g** The expression of miR-758-3p in circRBM33-repressed HeLa and SiHa cells was determined via qRT-PCR. $^{*}P < 0.05$

observed that the increase of miR-758-3p in si-circRBM33-transfected HeLa and SiHa cells was restored after transfection with anti-miR-758-3p (Fig. 4a). Moreover, miR-758-3p downregulation abolished circRBM33 inhibition-mediated influence on proliferation, apoptosis, migration, and invasion of HeLa and SiHa cells (Fig. 4b, f). Furthermore, the downregulation of N-cadherin and Vimentin and the upregulation of E-cadherin in circRBM33-inhibited HeLa and SiHa cells were overturned by miR-758-3p silencing (Fig. 4g, h). Additionally, the silence of miR-758-3p abrogated the repressive impact of circRBM33 knockdown on glucose consumption and lactate production of HeLa and SiHa cells (Fig. 4i, j). Also, miR-758-3p silencing reversed the downregulation of HK2 protein in circRBM33-silenced HeLa and SiHa cells (Fig. 4k, l). These data suggested that circRBM33 played its function in CC cells via sponging miR-758-3p.

PUM2 severed as a downstream target of miR-758-3p in CC

To deeply explore the underlying mechanism of miR-758-3p in CC, we predicted the possible targets for miR-758-3p with the targetscan database. The results presented that PUM2 might be a target of miR-758-3p (Fig. 5a). Moreover, the luciferase activity of the luciferase vector with PUM2 3′-UTR-WT was repressed by miR-758-3p mimic, while there was no overt difference in the luciferase activity of luciferase vector with PUM2 3′-UTR-MUT (Fig. 5b, c). We also observed that the levels of PUM2 mRNA and protein were increased in CC tissues (Fig. 5d, e). Consistently, the levels of PUM2 mRNA and protein were elevated in CC cells (HeLa and SiHa) (Fig. 5f, g). Also, the forcing expression of miR-758-3p constrained decreased the levels of

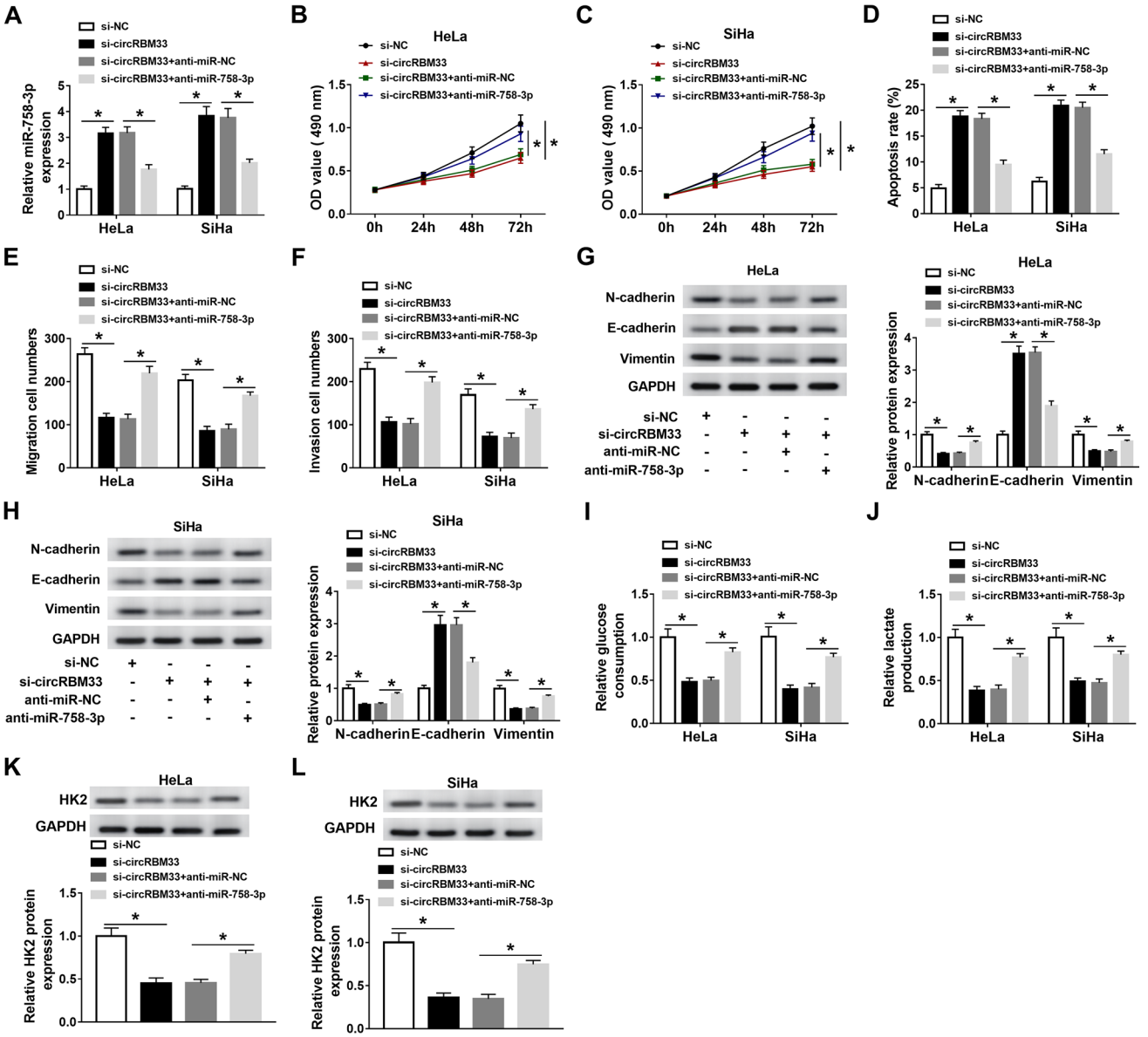

Fig. 4 CircRBM33 modulated CC progression through absorbing miR-758-3p. **a**–**j** HeLa and SiHa cells were transfected with si-NC, si-circRBM33, si-circRBM33 + anti-miR-NC, or si-circRBM33 + anti-miR-758-3p. **a** The expression of miR-758-3p in HeLa and SiHa cells was analyzed with qRT-PCR. **b**–**f** The proliferation, apoptosis, migration, and invasion of HeLa and SiHa cells were assessed via MTT assay, flow cytometry assay, or transwell assay. **g**, **h** The levels of E-cadherin, N-cadherin, and Vimentin in HeLa and SiHa cells were measured by western blotting. **i**, **j** The levels of glucose consumption and lactate production in HeLa and SiHa cells were analyzed with special commercial kits. **k**, **l** The levels of HK2 protein in HeLa and SiHa cells were examined with western blotting. $^{*}P < 0.05$

PUM2 mRNA and protein in HeLa and SiHa cells (Fig. 5h, i). Collectively, these findings indicated that miR-758-3p targeted PUM2 in CC cells.

MiR-758-3p repressed CC cell malignancy and glycolysis by targeting PUM2 in vitro

In light of the above findings, we further analyzed whether miR-758-3p targeted PUM2 to regulate the progression of CC. The downregulation of PUM2 mRNA and protein in miR-758-3p-overexpressed HeLa and SiHa cells was restored after PUM2 overexpression (Fig. 6a, b). Moreover, the forcing expression of miR-758-3p repressed proliferation, migration, invasion, and facilitated apoptosis of HeLa and SiHa cells, but these impacts were overturned by PUM2 overexpression (Fig. 6c, g). Subsequently, we observed that the downregulation of N-cadherin and Vimentin and the upregulation of E-cadherin in miR-758-3p-elevated HeLa

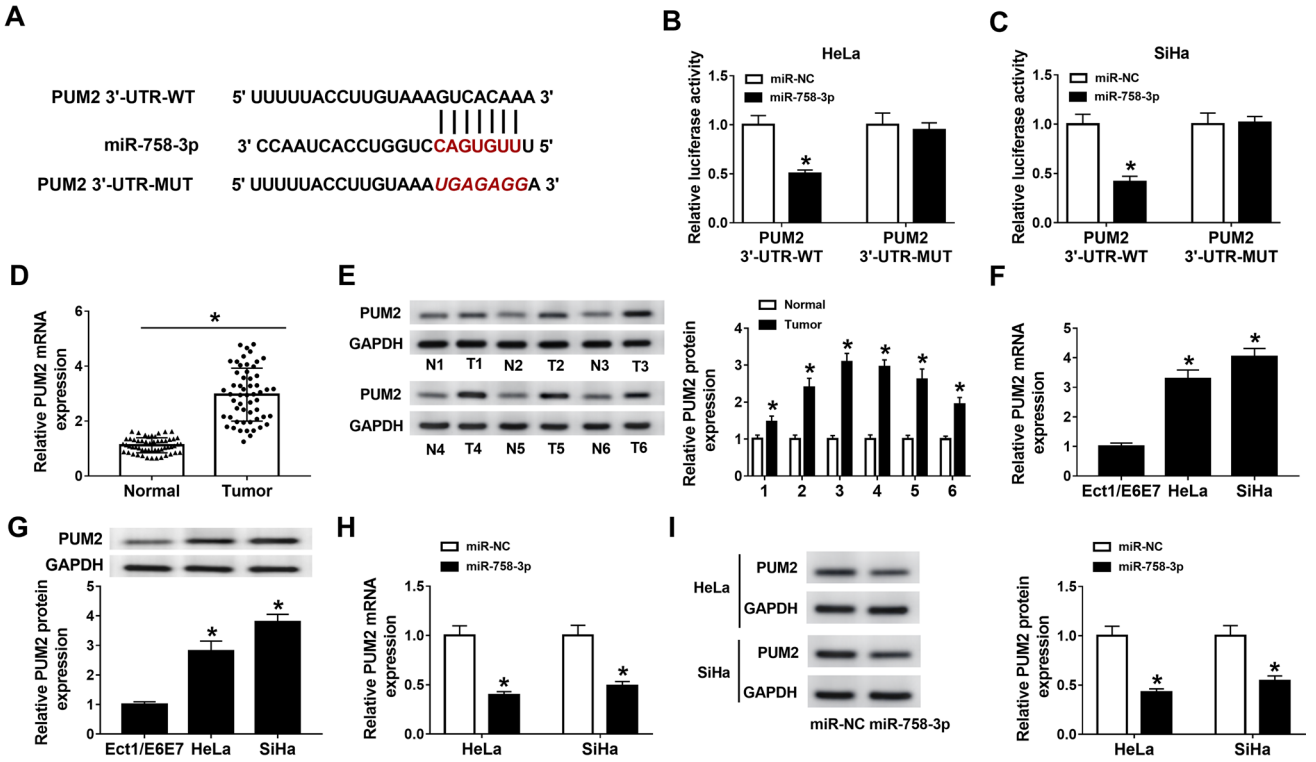

Fig. 5 PUM2 acted as a target for miR-758-3p in CC. **a** Schematic diagram of the binding sites between PUM2 and miR-758-3p. **b**, **c** Dual-luciferase reporter assay was conducted for the evaluation of the luciferase intensity in HeLa and SiHa cells co-transfected with luciferase vector containing PUM2 3′-UTR-WT or PUM2 3′-UTR-MUT and miR-NC or miR-758-3p. **d**–**g** The levels of PUM2 mRNA and protein in CC tissues and cells (HeLa and SiHa) were measured through qRT-PCR or western blotting. **h**, **i** The levels of PUM2 mRNA and protein in HeLa and SiHa cells transfected with miR-NC or miR-758-3p were determined via qRT-PCR or western blotting. $^{*}P < 0.05$

and SiHa cells were reversed by PUM2 overexpression (Fig. 6h, i). Also, the decrease of glucose consumption and lactate production in miR-758-3p-overexpressed HeLa and SiHa cells was restored by PUM2 elevation (Fig. 6j, k). Furthermore, the downregulation of HK2 protein in HeLa and SiHa cells induced by miR-758-3p elevation was abolished after PUM2 overexpression (Fig. 6l, m). Taken together, these results manifested that miR-758-3p regulated CC progression via targeting PUM2.

CircRBM33 sponged miR-758-3p to regulate PUM2 expression

Based on the above results, we further analyzed whether circRBM33 functioned as a ceRNA to regulate PUM2 expression via sponging miR-758-3p. The results exhibited that the knockdown of circRBM33 reduced the levels of PUM2 mRNA and protein in HeLa and SiHa cells, while this decrease was reversed by miR-758-3p inhibition (Fig. 7a, b). These data suggested that circRBM33 regulated the expression of PUM2 via sponging miR-758-3p in CC cells.

CircRBM33 knockdown constrained tumor growth in vivo

Subsequently, we further verified the function of circRBM33 in CC through tumor formation experiments. The results exhibited that circRBM33 knockdown reduced tumor volume and weight when compared with the sh-NC group (Fig. 8a, b). Moreover, circRBM33 was downregulated while miR-758-3p was upregulated in mice tumor tissues of the sh-circRBM33 group in contrast to the sh-NC group (Fig. 8c, d). Also, the levels of PUM2 mRNA and protein were decreased in mice tumor tissues of the sh-circRBM33 group than that in the sh-NC group (Fig. 8e, f). Together, these results indicated that circRBM33 inhibition decreased CC growth in vivo.

Discussion

CC has a high morbidity and mortality rate, which threatens the health of woman worldwide (Torre et al. 2015). CircRNAs have been proved to play an important role in human

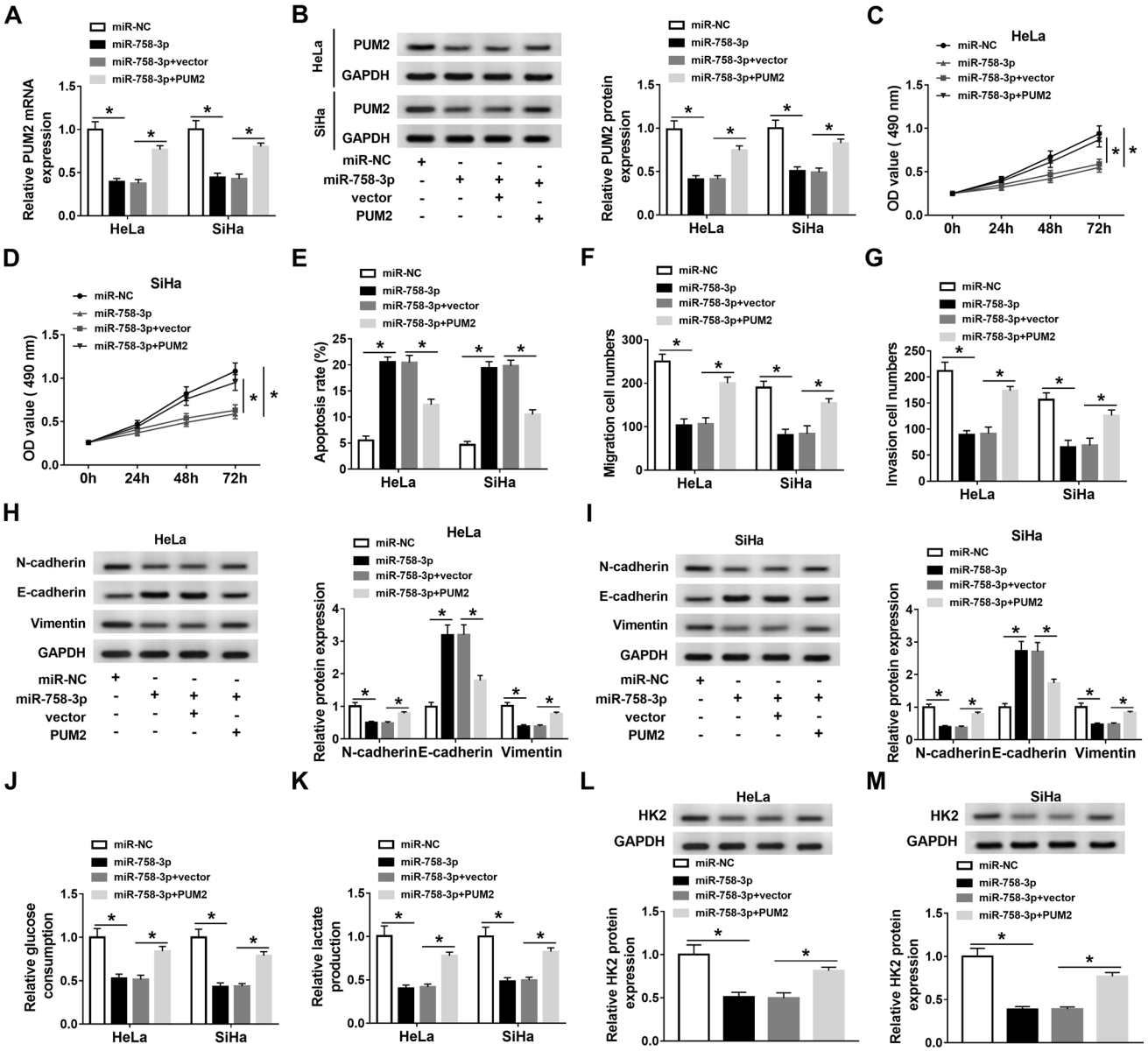

Fig. 6 MiR-758-3p modulated CC progression by targeting PUM2. **a**–**m** HeLa and SiHa cells were transfected with miR-758-3p, miR-NC, miR-758-3p + vector, or miR-758-3p + PUM2. **a**, **b** QRT-PCR and western blotting were conducted for the assessment of the levels of PUM2 mRNA or protein in HeLa and SiHa cells. **c**–**g** The proliferation, apoptosis, migration, and invasion of HeLa and SiHa cells were determined through MTT assay, flow cytometry assay, or transwell assay. **h**, **i** Western blotting was performed to measure the levels of E-cadherin, N-cadherin, and Vimentin in HeLa and SiHa cells. **j**, **k** The levels of glucose consumption and lactate production in HeLa and SiHa cells were detected with corresponding commercial kit. (l and m) Western blotting was carried out to evaluate the level of HK2 protein in HeLa and SiHa cells. $^{*}P < 0.05$

cancer (Kristensen et al. 2018). For instance, circRNA BCRC-3 repressed bladder cancer progression via enhancing p27 expression through sponging miR-182-5p (Xie et al. 2018). CircRNA circTADA2A sponged miR-203a to elevate CREB3 expression, which accelerated osteosarcoma advancement (Wu et al. 2019a, b). Increasing evidence had demonstrated that circRNAs participated in the progression of CC. Hsa_circ_101996 contributed to CC progression through regulating the miR-8075/TPX2 pathway (Wu et al. 2019a, b). Hsa_circ_0007534 promoted cell invasion and proliferation through the miR-498/BMI-1 pathway in CC (Rong et al. 2019). Herein, we verified that circRBM33 expression was increased in CC tissues and cells, and high circRBM33 expression had a shorter overall survival, indicating that circRBM33 might be a prognostic biomarker. CircRBM33 inhibition contributed to cell apoptosis and

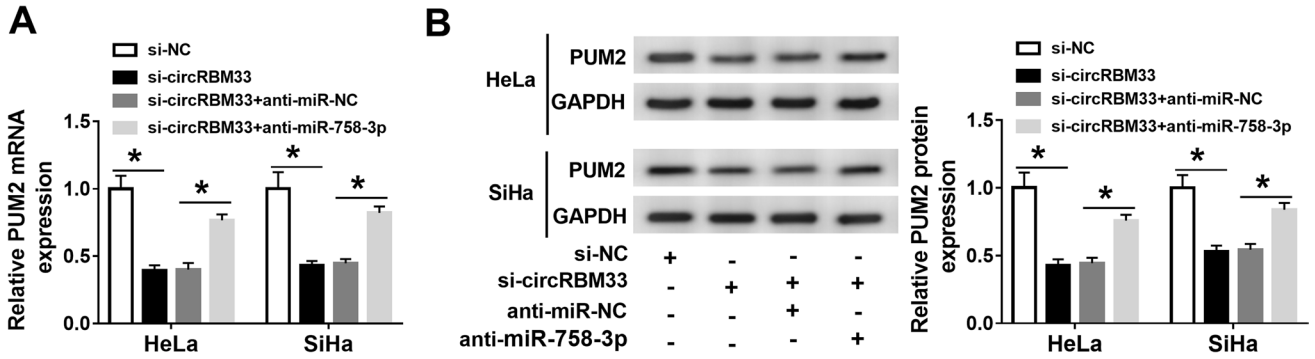

Fig. 7 CircRBM33 regulated PUM2 expression through sponging miR-758-3p in CC cells. **a**, **b** The levels of PUM2 mRNA and protein in HeLa and SiHa cells transfected with si-NC, si-circRBM33, si-circRBM33 + anti-miR-NC, or si-circRBM33 + anti-miR-758-3p were detected via qRT-PCR or western blotting. $^*P < 0.05$

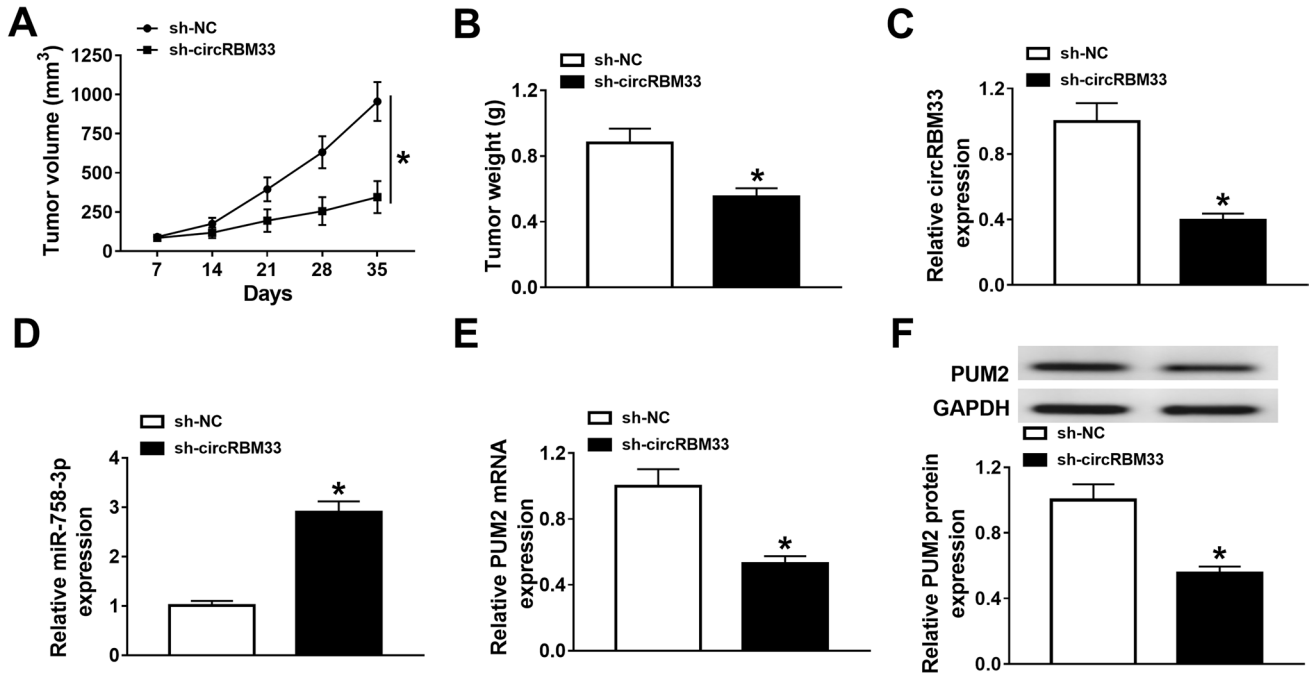

Fig. 8 CircRBM33 knockdown repressed tumor growth in vivo. **a** Tumor growth curves of the sh-circRBM33 and sh-NC groups. **b** Tumor weight of the sh-circRBM33 and sh-NC groups on day 35 after injection. **c**–**f** The levels of circRBM33, miR-758-3p, and PUM2 (mRNA and protein) in mice tumor tissues of the sh-circRBM33 and sh-NC groups were analyzed by qRT-PCR or western blotting. $^*P < 0.05$

constrained cell proliferation, migration, invasion, and glycolysis in CC cells. Also, circRBM33 knockdown constrained tumor growth in vivo. A recent study stated that circRBM33 silencing facilitated cell apoptosis and suppressed cell invasion, migration, and proliferation in gastric cancer cells through inhibition of IL-6 expression via absorbing miR-149 (Wang et al. 2020). Therefore, these data indicated that circRBM33 acted as an unfavorable regulator in CC.

A series of evidence had manifested that circRNA could modulate gene expression via sponging miRNA (Ren et al. 2019; Tang et al. 2019; Yao et al. 2019). CircRNA LDLRAD3 modulated pancreatic cancer development by regulating PTN expression through sponging miR-137-3p (Yao et al. 2019). In this study, we discovered that circRBM33 served as a sponge for miR-758-3p in CC cells. Previous research had pointed out that miR-758-3p elevation curbed hepatocellular cancer advancement through suppression of MDM2 and mTOR expression (Jiang et al. 2017). MiR-758-3p could repressed bladder cancer development via targeting NOTCH2 (Wu et al. 2019a, b). Hu et al. manifested that CASC9 facilitated the malignancy of ovarian cancer cells by suppressing miR-758-3p expression

(Hu et al. 2019). Our research revealed that miR-758-3p was downregulated in CC tissues and cells. MiR-758-3p silencing overturned circRBM33 silencing-mediated impacts on the malignant behaviors of CC cells. Meng et al. also pointed out that miR-758-3p expression was reduced in CC (Meng et al. 2017). Furthermore, miR-758-3p repressed cell metastasis and proliferation through targeting HMGB3 in CC (Song et al. 2019). These data manifested that miR-758-3p played a tumor repressive role in CC, and circRBM33 accelerated CC progression through sponging miR-758-3p.

In addition, we found that PUM2 served as a target for miR-758-3p in CC cells. In breast cancer, PUM2 facilitated cell stemness by competitively binding to NRP-1 with miR-376a (Zhang et al. 2019). PUM2 could contribute to glioblastoma progression by repression of BTG1 expression (Wang et al. 2019). Duan et al. indicated that TUG1 aggravated CC progression via interacting with PUM2 (Duan et al. 2019). Herein, PUM2 was upregulated in CC tissues and cells, and PUM2 elevation overturned the inhibitory influence of miR-758-3p overexpression on the malignant behaviors of CC cells, manifested that PUM2 acted as an oncogene in CC. Besides, Hu et al. revealed that PUM2 was downregulated in osteosarcoma tissues, and PUM2 competed to bind to STARD13 with miR-9 and miR-590-3p and repressed osteosarcoma progression, which might be related to tissue specificity (Hu et al. 2018). Furthermore, circRBM33 regulated PUM2 expression through absorbing miR-758-3p in CC cells. Therefore, we concluded that circRBM33 modulated CC progression through regulation of PUM2 expression via sponging miR-758-3p.

In summary, circRBM33 played a tumor promoting role in CC. circRBM33 facilitated CC development through modulation of the miR-758-3p/PUM2 axis. This work indicated that circRBM33 might be a promising target for the treatment of CC.

Acknowledgements None.

Funding This work was supported by the Social and Development Project of Changzhou (Grant No. CE20175004).

Compliance with ethical standards

Conflict of interest The authors declare that they have no conflicts of interest.

References

Bray F, Ferlay J, Soerjomataram I, Siegel RL, Torre LA, Jemal A (2018) Global cancer statistics 2018: GLOBOCAN estimates of incidence and mortality worldwide for 36 cancers in 185 countries. Cancer J Clin 68(6):394–424

Chen B, Huang S (2018) Circular RNA: an emerging non-coding RNA as a regulator and biomarker in cancer. Cancer Lett 418:41–50

Chen D, Ma W, Ke Z, Xie F (2018) CircRNA hsa_circ_100395 regulates miR-1228/TCF21 pathway to inhibit lung cancer progression. Cell Cycle (Georgetown Tex) 17(16):2080–2090

Chen J, Xu Z, Yu C, Wu Z, Yin Z, Fang F, Chen B (2019) MiR-758-3p regulates papillary thyroid cancer cell proliferation and migration by targeting TAB1. Pharmazie 74(4):235–238

Di Leva G, Garofalo M, Croce CM (2014) MicroRNAs in cancer. Annu Rev Pathol 9:287–314

Duan W, Nian L, Qiao J, Liu NN (2019) LncRNA TUG1 aggravates the progression of cervical cancer by binding PUM2. Eur Rev Med Pharmacol Sci 23(19):8211–8218

Feng S, Liu W, Bai X, Pan W, Jia Z, Zhang S, Zhu Y, Tan W (2019) LncRNA-CTS promotes metastasis and epithelial-to-mesenchymal transition through regulating miR-505/ZEB2 axis in cervical cancer. Cancer Lett. 465:105–117

Hsiao K-Y, Sun HS, Tsai S-J (2017) Circular RNA—new member of noncoding RNA with novel functions. Exp Biol Med (Maywood, NJ) 242(11):1136–1141

Hu R, Zhu X, Chen C, Xu R, Li Y, Xu W (2018) RNA-binding protein PUM2 suppresses osteosarcoma progression via partly and competitively binding to STARD13 3'UTR with miRNAs. Cell Prolif 51(6):e12508

Hu X, Li Y, Kong D, Hu L, Liu D, Wu J (2019) Long noncoding RNA CASC9 promotes LIN7A expression via miR-758-3p to facilitate the malignancy of ovarian cancer. J Cell Physiol 234(7):10800–10808

Jiang D, Cho W, Li Z, Xu X, Qu Y, Jiang Z, Guo L, Xu G (2017) MiR-758-3p suppresses proliferation, migration and invasion of hepatocellular carcinoma cells via targeting MDM2 and mTOR. Biomed Pharmacother Biomedpharmacother 96:535–544

Kodama J, Seki N, Masahiro S, Kusumoto T, Nakamura K, Hongo A, Hiramatsu Y (2010) Prognostic factors in stage IB-IIB cervical adenocarcinoma patients treated with radical hysterectomy and pelvic lymphadenectomy. J Surg Oncol 101(5):413–417

Kristensen LS, Hansen TB, Venø MT, Kjems J (2018) Circular RNAs in cancer: opportunities and challenges in the field. Oncogene 37(5):555–565

Li N, Miao Y, Shan Y, Liu B, Li Y, Zhao L, Jia L (2017) MiR-106b and miR-93 regulate cell progression by suppression of PTEN via PI3K/Akt pathway in breast cancer. Cell Death Dis 8(5):e2796

Meng X, Zhao Y, Wang J, Gao Z, Geng Q, Liu X (2017) Regulatory roles of miRNA-758 and matrix extracellular phosphoglycoprotein in cervical cancer. Exp Ther Med 14(4):2789–2794

Ren S, Liu J, Feng Y, Li Z, He L, Li L, Cao X, Wang Z, Zhang Y (2019) Knockdown of circDENND4C inhibits glycolysis, migration and invasion by up-regulating miR-200b/c in breast cancer under hypoxia. J Exp Clin Cancer Res CR 38(1):388

Rischin D, Narayan K, Oza AM, Mileshkin L, Bernshaw D, Choi J, Hicks R, McClure B, Fyles A (2010) Phase 1 study of tirapazamine in combination with radiation and weekly cisplatin in patients with locally advanced cervical cancer. Int J Gynecol Cancer Off J Int Gynecol Cancer Soc 20(5):827–833

Rong X, Gao W, Yang X, Guo J (2019) Downregulation of hsa_circ_0007534 restricts the proliferation and invasion of cervical cancer through regulating miR-498/BMI-1 signaling. Life Sci 235:116785

Rui X, Xu Y, Jiang X, Ye W, Huang Y, Jiang J (2018) Long non-coding RNA C5orf66-AS1 promotes cell proliferation in cervical cancer by targeting miR-637/RING1 axis. Cell Death Dis 9(12):1175

Rupaimoole R, Slack FJ (2017) MicroRNA therapeutics: towards a new era for the management of cancer and other diseases. Nat Rev Drug Discov 16(3):203–222

Song T, Hou X, Lin B (2019) MicroRNA-758 inhibits cervical cancer cell proliferation and metastasis by targeting HMGB3 through the WNT/β-catenin signaling pathway. Oncol Lett 18(2):1786–1792

Tang Q, Chen Z, Zhao L (2019) Circular RNA hsa_circ_0000515 acts as a miR-326 sponge to promote cervical cancer progression through up-regulation of ELK1. Aging 11(22):9982–9999

Torre LA, Bray F, Siegel RL, Ferlay J, Lortet-Tieulent J, Jemal A (2015) Global cancer statistics, 2012. CA Cancer J Clin 65(2):87–108

Wang Y, Sun W, Yang J, Yang L, Li C, Liu H, Liu X, Jiao B (2019) PUM2 promotes glioblastoma cell proliferation and migration via repressing BTG1 expression. Cell Struct Funct 44(1):29–39

Wang N, Lu K, Qu H, Wang H, Chen Y, Shan T, Ge X, Wei Y, Zhou P, Xia J (2020) CircRBM33 regulates IL-6 to promote gastric cancer progression through targeting miR-149. Biomed Pharmacother Biomed Pharmacother 125:109876

Wu X, Chen B, Shi H, Zhou J, Zhou F, Cao J, Sun X (2019) miR-758-3p suppresses human bladder cancer cell proliferation, migration and invasion by targeting NOTCH2. Exp Ther Med 17(5):4273–4278

Wu Y, Xie Z, Chen J, Chen J, Ni W, Ma Y, Huang K, Wang G, Wang J, Ma J, Shen S, Fan S (2019) Circular RNA circTADA2A promotes osteosarcoma progression and metastasis by sponging miR-203a-3p and regulating CREB3 expression. Mol Cancer 18(1):73

Xie F, Li Y, Wang M, Huang C, Tao D, Zheng F, Zhang H, Zeng F, Xiao X, Jiang G (2018) Circular RNA BCRC-3 suppresses bladder cancer proliferation through miR-182-5p/p27 axis. Mol Cancer 17(1):144

Yao J, Zhang C, Chen Y, Gao S (2019) Downregulation of circular RNA circ-LDLRAD3 suppresses pancreatic cancer progression through miR-137-3p/PTN axis. Life Sci 239:116871

Zhang J-J, Wang D-D, Du C-X, Wang Y (2018) Long noncoding RNA ANRIL promotes cervical cancer development by acting as a sponge of miR-186. Oncol Res 26(3):345–352

Zhang S, McNamara M, Batur P (2018) Cervical cancer screening: what's new? Updates for the busy clinician. Am J Med 131(6):702.e701-702.e705

Zhang L, Chen Y, Li C, Liu J, Ren H, Li L, Zheng X, Wang H, Han Z (2019) RNA binding protein PUM2 promotes the stemness of breast cancer cells via competitively binding to neuropilin-1 (NRP-1) mRNA with miR-376a. Biomed Pharmacother Biomed Pharmacother 114:108772